(Preprint) AAS 11-215

METHODS OF OPTICAL NAVIGATION*

William M. Owen, Jr.†

Optical navigation is the use of onboard imaging to aid in the determination of the spacecraft trajectory and of the targets' ephemerides. Opnav techniques provide a direct measurement of the direction from a spacecraft to target bodies. Opnav data thus complement both radiometric tracking data (for instance, Doppler and range) and the groundbased astrometry which is used to determine the *a priori* ephemeris of the targets.

We present the geometry and camera models which form the mathematical basis for optical navigation and some of the image processing techniques by which one can extract the optical observables—that is, the sample and line coordinates of images—from pictures.

INTRODUCTION

Optical navigation ("opnav")[1] is the use of imaging data to aid in spacecraft navigation. In the typical case, a camera on a spacecraft takes a picture of some nearby target body. The spacecraft's attitude determination system provides an estimate of the attitude of the camera during the exposure; star images, if present in the picture, serve to improve the attitude knowledge. Then an accurate measurement of the image coordinates of the target become in effect a measurement of the inertial direction from the camera to the target: a unit vector, with no distance information.

A succession of opnav pictures or the presence of multiple targets within one picture *can* provide some measurement of distance; pictures taken at right angles can provide a reliable position fix.[2] Still, the essence of opnav is that the information it provides is target-relative.

Groundbased astrometry, radar ranging, and other historical tracking data determine the heliocentric position and velocity of the target bodies. Radiometric tracking data (Doppler, range, and ΔDOR) alone are sufficient to provide the heliocentric position and velocity of a spacecraft. If the target is sufficiently massive, radiometric data will also be sensitive to the spacecraft's position relative to the target, but there is no such sensitivity in the case of comets or small asteroids. For these small bodies, only optical data (or its close relative, altimetry) can provide a direct measure of the spacecraft's position with respect to the target.

The practice of optical navigation consists of two quite different problems and a third problem closely related to the first.

1) Given the position and velocity of the spacecraft and the target, the camera attitude, and the camera's optical properties, where should the image of the target appear within a picture? To solve this problem requires little more than basic three-dimensional analytic geometry coupled with geometric optics.

2) Given a digital picture containing images of targets or stars, what are the measured coordinates of these images? The solution to this second problem lies in the realm of image processing; one typically produces a model of the expected brightness distribution and fits the model to the picture.

3) Even after the image processing is done and the measured coordinates are in hand, the work of the opnav analyst is not complete. The measurements must be fed into the orbit determination filtering process. One must therefore compute not only the measurement residuals—a repeat of the first problem— but also the

†Supervisor, Optical Navigation Group, Jet Propulsion Laboratory, California Institute of Techology, 4800 Oak Grove Drive, Pasadena CA 91109-8099 USA

partial derivatives of the computed measurements with respect to all the parameters of the OD process. The partials are easily obtained by differentiating the geometry equations.

This paper treats all three problems.

Within this paper, scalar quantities appear in *italics*, vectors in **boldface**, and matrices in **boldface sans-serif**. Special terms appear in *slanted* type at their first appearance in the text. Superscripts to vectors or matrices indicate the coordinate system in which their components are expressed.

OPNAV GEOMETRY

The goal of the optical navigation prediction process is to determine the expected coordinates of the *image* of some sort of *target* within a *picture* taken by a *camera*.

A target can be anything. In traditional opnav, targets typically are the coordinate centers of nearby Solar System objects: planetary satellites, asteroids, comets, and occasionally the planets themselves. Targets may also include features or "landmarks" on the surface of a body, even another spacecraft. Stars are also considered targets, because it is important to measure their images too.

A camera is some device capable of producing a picture. In effect, it maps a direction in its own coordinate system onto a point in the plane of the picture. Again in traditional opnav, the camera is carried on a spacecraft, and the pictures it acquires are used to navigate the spacecraft. There is, however, no need to assume a spacecraft: the camera can be anywhere.

The problem of predicting the location of the image of a target within a picture therefore has three components: determining the inertial direction from the camera to the target, determining the orientation (attitude) of the camera with respect to inertial coordinates, and applying the camera mapping or projection to determine the image coordinates corresponding to a given direction.

The equations presented here have their basis in photographic astrometry, a field which dates to the latter part of the 19th century. König[3] has provided a review of that field.

Inertial Direction to a Target

Because optical navigation uses images, and images are produced by photons emanating from a target, the direction of interest is not the "actual" or *geometric* position vector but rather the *apparent* position vector, the direction from which the photons appear to come. The formulation below follows standard astronomical practice, as documented in the *Explanatory Supplement to the Astronomical Almanac*[4] and elsewhere. The calculations assume an inertial reference frame I: nonrotating, with an unaccelerated origin.

Targets within the Solar System. One finds the apparent vector as follows:

1) Compute the position $\mathbf{R}^{\mathrm{I}}(t)$ and velocity $\dot{\mathbf{R}}^{\mathrm{I}}(t)$ of the camera at the time t corresponding to the midpoint of the exposure. These vectors are referred to the barycenter of the Solar System.

2) Compute the position $\mathbf{S}^{\mathrm{I}}(t)$ of the target similarly.

3) The difference $\mathbf{G}(t) = \mathbf{S}(t) - \mathbf{R}(t)$ is the *geometric* relative position. If the speed of light c were infinite, $\mathbf{G}(t)$ would also represent the observed position.

4) Because c is not infinite, the camera sees the target not as it is during the exposure, but as it was at the *retarded time* $t' = t - \tau$, where τ, the *light time*, is the time required for light to travel from the target to the camera:

$$\tau = |\mathbf{R}(t) - \mathbf{S}(t - \tau)|/c. \tag{1}$$

As τ appears on both sides of Eq. (1), this equation must be solved iteratively. Two iterations suffice.

5) The *true* position $\mathbf{T}(t)$ of the target, now corrected for light time, is

$$\mathbf{T}(t) = \mathbf{R}(t) - \mathbf{S}(t - \tau). \tag{2}$$

6) If the camera were at rest relative to the Solar System barycenter, Eq. (1) would provide the direction from which the camera detects the incoming light. Stellar aberration, however, shifts this direction toward the *velocity apex* of the camera. The *apparent* position $\mathbf{A}(t)$ is found most easily by a vector addition:

$$\mathbf{A}(t) = \mathbf{T}(t) + |\mathbf{T}(t)|\,[\dot{\mathbf{R}}(t)/c]. \tag{3}$$

This equation represents the Newtonian formulation, which is sufficient for optical navigation purposes. A formulation compatible with special relativity may be found in Stumpff.[5]

Stars. The formulation for stars is a bit simpler, as star catalogs already provide the equivalent of a true position. Catalogs typically provide the *right ascension* $\alpha(t_\alpha)$ at some time t_α, the *declination* $\delta(t_\delta)$ similarly, and the *proper motion* components μ_α and μ_δ, which are $d\alpha/dt$ and $d\delta/dt$ respectively. Note that R.A. is commonly measured not in degrees but in *hours*, minutes, and seconds "of time," with $24^{\mathrm{h}} \equiv 360^\circ$. Furthermore, many catalogs provide not μ_α itself but rather $\mu_\alpha^* \equiv \mu_\alpha \cos\delta$, typically measured in the same units (*e.g.*, arc seconds per year) as μ_δ. One must read each catalog's documentation carefully. Currently the HIPPARCOS catalog[6] is the realization of the International Celestial Reference Frame at optical wavelengths. Subsequent catalogs such as Tycho-2 or UCAC2, both reduced to HIPPARCOS, provide a denser, fainter set of stars.[7,8]

1a) For most stars, the proper motion may be considered constant. One therefore computes

$$\alpha(t) = \alpha(t_\alpha) + (t - t_\alpha)\mu_\alpha \tag{4}$$

and similarly for $\delta(t)$. It is not uncommon for t_α and t_δ to be different. The angular coordinates, combined with the distance d, yield the star's position vector

$$\mathbf{S}^{\mathrm{I}}(t) = d \begin{pmatrix} \cos\alpha(t)\cos\delta(t) \\ \sin\alpha(t)\cos\delta(t) \\ \sin\delta(t) \end{pmatrix} \tag{5}$$

relative to the barycenter of the Solar System. Note that catalogs often provide not a star's distance but its *parallax* $\pi \equiv 1$ parsec$/d$. If the distance is unknown, one should set it to some very large number.

1b) For some nearby stars with large proper motions, and for some stars very close to a celestial pole, the above approximation can break down. A better approach takes the star's *space velocity* $\mathbf{V}^{\mathrm{I}}$ to be constant, yielding rectilinear motion:

$$\mathbf{S}^{\mathrm{I}}(t) = \mathbf{S}^{\mathrm{I}}(t_0) + (t - t_0)\mathbf{V}^{\mathrm{I}}. \tag{6}$$

This approach presumes that the star's distance and radial velocity are known. Details are found in the *Explanatory Supplement*[4] or in section 1.2.8 of Volume 1 of the HIPPARCOS documentation.[6]

2) As light time is already included in the coordinates of the star, it suffices to form

$$\mathbf{T}(t) = \mathbf{S}(t) - \mathbf{R}(t) \tag{7}$$

and then account for stellar aberration by Eq. (3).

Camera Attitude

The second aspect of the optical navigation geometry problem is the determination of attitude of the camera. Define a camera-fixed Cartesian coordinate system M-N-L such that the L-axis is the *optical axis* of the camera, with $+L$ pointing away from the camera toward the scene being imaged. The M- and N-axes are perpendicular to the optical axis. The directions of M and N are arbitrary; JPL usage (Figure 1) has $+M$ pointing to the left and $+N$ up, from a vantage point behind the camera. This produces a right-handed coordinate system C.

The transformation from inertial coordinates to camera coordinates is effected by a rotation matrix C. An apparent vector $\mathbf{A}^{\mathrm{I}}$, expressed in inertial coordinates, is transformed into camera coordinates to become the vector $\mathbf{A}^{\mathrm{C}}$ by

$$\mathbf{A}^{\mathrm{C}} = \mathsf{C}\,\mathbf{A}^{\mathrm{I}}. \tag{8}$$

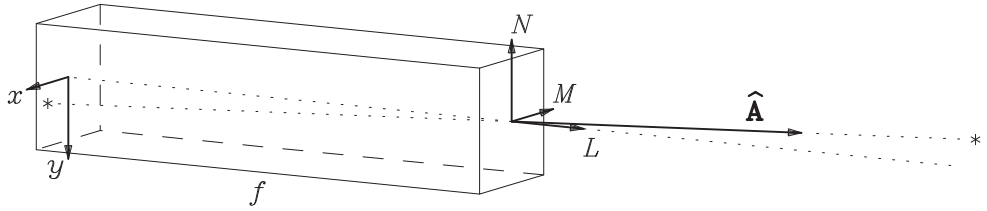

Figure 1. A pinhole camera showing the gnomonic projection for a star.

This transformation does not change the direction in which the vector points; it merely changes the coordinate system in which its components are expressed.

The goal is to find the full matrix $\mathbf{C}$, not merely the direction of the optical axis (the third row of $\mathbf{C}$). There are many ways to proceed, some of them mission specific.

The simplest is to write the rotation as a sequence of three elementary rotations by Euler angles, such as

$$\mathbf{C} = \mathbf{R}_3(\phi)\,\mathbf{R}_1(90^\circ - \delta)\,\mathbf{R}_3(\alpha + 90^\circ) \tag{9}$$

or

$$\mathbf{C} = \mathbf{R}_3(\phi')\,\mathbf{R}_2(90^\circ - \delta)\,\mathbf{R}_3(\alpha) \tag{10}$$

with $\phi' = \phi + 90^\circ$. The expression $\mathbf{R}_i(\theta)$ denotes a rotation of the coordinate axes by angle θ about the ith axis. For instance,

$$\mathbf{R}_1(\theta) = \begin{pmatrix} 1 & 0 & 0 \\ 0 & \cos\theta & \sin\theta \\ 0 & -\sin\theta & \cos\theta \end{pmatrix}. \tag{11}$$

In Eqs. (9) and (10), α and δ are by construction the right ascension and declination of the optical axis ($+L$), and ϕ or ϕ' a twist angle.

Either of the preceding formulations is appropriate when the camera attitude is available from spacecraft telemetry or when all three angles are controllable. Often, however, the camera has only two degrees of freedom, not three: the spacecraft architecture or operating constraints force the camera to one possible orientation given the pointing direction. That is, $\phi = f(\alpha, \delta)$. Usually there will exist some "azimuth/elevation" coordinate system A in which the camera attitude is specified by two rotations. If the orientation of A with respect to inertial coordinates is specified by a rotation matrix $\mathbf{A}$, the camera attitude is then

$$\mathbf{C} = \mathbf{R}_2(e)\,\mathbf{R}_3(a)\,\mathbf{A} \tag{12}$$

where a and e are the azimuth and elevation angles. These are found by rotating the desired pointing direction $\hat{\mathbf{L}}$ from inertial coordinates into A:

$$\begin{pmatrix} \cos a \sin e \\ \sin a \sin e \\ \cos e \end{pmatrix} = \mathbf{A}\,\hat{\mathbf{L}}^{\mathrm{I}}. \tag{13}$$

Camera Projection

An ideal camera acts as if the lens were a point. Light rays from a target pass through that point, which we take to be the origin of the camera coordinate system C, and continue in a straight line until they impinge upon a *detector*, which lies in a *focal plane* at a distance f from the origin. This process forms a *real image* on the detector. In this model, the line through the origin perpendicular to the detector defines the optical axis, and f is the *focal length* of the camera.

The image of a target at apparent position $\mathbf{A}^{\mathrm{C}}$ (expressed in camera coordinates) appears on the detector, *inverted* or "upside-down," at coordinates (x, y). The simple geometry of the *gnomonic projection* (Figure 1) shows that

$$\begin{pmatrix} x \\ y \end{pmatrix} = \frac{f}{A_3^{\mathrm{C}}} \begin{pmatrix} A_1^{\mathrm{C}} \\ A_2^{\mathrm{C}} \end{pmatrix}. \tag{14}$$

Because the right hand side of Equation (14) involves ratios of the components of $\mathbf{A}$, the magnitude of $\mathbf{A}$ is irrelevant. The units of x and y are the same as those of f, typically millimeters. Note that the x- and y-axes, used for measuring image coordinates, are by convention antiparallel to the M- and N-axes of the camera body, in order to avoid introducing minus signs into the model.

Real cameras, whether by design or through misalignment, are not ideal. The breakdown of the small-angle approximation $\sin\theta \approx \tan\theta \approx \theta$ introduces *aberrations* into an optical system. The details of geometrical optics are beyond the scope of this paper; readers are referred to textbooks such as Schroeder's *Astronomical Optics*[9] or Jenkins and White's *Fundamentals of Optics*.[10] For optical navigation purposes, what is important is that navigators be able to model the effects of imperfect optical systems on the locations of images. The three dominant terms arise from *cubic radial distortion* (one of the five third-order aberrations) and *tip and tilt misalignments*.

Radial distortion displaces images radially, toward or away from the optical axis, by an amount proportional to the cube of the distance from the optical axis. The displacement is resolved into x and y components, giving

$$\begin{pmatrix}\Delta x\\ \Delta y\end{pmatrix} = \epsilon_1 \begin{pmatrix}xr^2\\ yr^2\end{pmatrix} \tag{15}$$

where of course $r^2 \equiv x^2 + y^2$. The coefficient ϵ_1 yields *pincushion distortion* or *barrel distortion* according to whether it is positive or negative.

Tip and tilt terms arise when the detector is not perpendicular to the optical axis. The part of the detector which is further from the pinhole has in effect a longer focal length than nominal; the part which is closer seems to have a shorter focal length. The consequence is that the image of a square target is distorted into a trapezoid. There are two terms, as the misalignment has two degrees of freedom:

$$\begin{pmatrix}\Delta x\\ \Delta y\end{pmatrix} = \epsilon_2 \begin{pmatrix}xy\\ y^2\end{pmatrix} + \epsilon_3 \begin{pmatrix}x^2\\ xy\end{pmatrix}. \tag{16}$$

These three terms combine to give an expression for the corrected image locations (x', y'):

$$\begin{pmatrix}x'\\ y'\end{pmatrix} = \begin{pmatrix}x\\ y\end{pmatrix} + \begin{pmatrix}xr^2 & xy & x^2\\ yr^2 & y^2 & xy\end{pmatrix} \begin{pmatrix}\epsilon_1\\ \epsilon_2\\ \epsilon_3\end{pmatrix}. \tag{17}$$

The other third-order aberrations—spherical aberration, coma, astigmatism, and curvature of field—affect the *shape* of an image but not directly its *position*. Insofar as the image centerfinding process is insensitive to changes in the appearance of the image, these aberrations do not affect the opnav results. If however the image centers determined by the software do change systematically across the field of view, these systematic changes can often be absorbed in the camera calibration.

Transformation Into Pixel Coordinates

The coordinates (x', y') have units of length. What we measure in a picture are the *pixel coordinates*. A digital picture contains a rectangular array of numbers, each of which is a *pixel* (the term is a contraction of "picture element"). Nomenclature differs: the horizontal coordinate is referred to as the *column*, *sample* or (confusingly) the *pixel* coordinate, while the vertical direction is the *row* or *line* coordinate. (The "line" and "sample" terminology refers to TV cameras, which would sample the picture while doing line-by-line scans.) The first column is displayed at the left side of the picture, but there is no unanimity about the first line: some systems display it at the top of the picture, others at the bottom. The math is the same either way. Similarly, there is no agreement as to whether the first pixel has coordinates $(0, 0)$ or $(1, 1)$.

A pixel can also be thought of as a quadrilateral area on the detector. In the former sense, pixel coordinates must be integers; in the latter sense, pixel coordinates are continuous. We use the same terminology in either case, and the context determines which interpretation holds. This subsection treats pixels as a continuous coordinate system.

Charge-coupled devices, active pixel sensors, and other silicon-based detectors have much greater geometric stability than the Vidicon television cameras used through Voyager. A fairly simple linear transformation suffices to transform (x, y) into sample s and line l:

$$\begin{pmatrix} s \\ l \end{pmatrix} = \begin{pmatrix} K_x & K_{xy} \\ K_{yx} & K_y \end{pmatrix} \begin{pmatrix} x' \\ y' \end{pmatrix} + \begin{pmatrix} s_0 \\ l_0 \end{pmatrix}. \tag{18}$$

The matrix $\mathbf{K}$ contains the reciprocal of the pixel dimensions; its components are typically measured in pixels/mm. For an ideal detector with square pixels, $K_x = K_y$ and the off-diagonal terms are zero. If the pixels are rectangular, $K_x \neq K_y$; if they are not rectangular, $K_{xy} \neq -K_{yx}$. Notice that there can be a rotation implicit in $\mathbf{K}$ as well. The last term in Eq. (18) contains the (s, l) coordinates of the optical axis, where by definition $x = y = 0$.

It is clear that not all the parameters of the camera model are independent. What is actually measured is the *pixel scale* or the *angular* size of a pixel. Increasing the focal length or decreasing the physical size of the pixels will have the same effect: one pixel will subtend a smaller angle. One can combine Eqs. (14) and (18), ignoring distortion, to derive the pixel scale S_s in the sample direction,

$$S_s = K_x / f \text{ radians/pixel}, \tag{19}$$

and similarly for the pixel scale in the line direction, S_l. One cannot in general determine f and K_x separately only from image analysis; one needs additional information, such as the measured size of a pixel.

Similarly, a rotation implicit in the terms of $\mathbf{K}$ is effectively the same as a rotation of the camera body itself. To put it another way, if an image appears rotated, one cannot tell whether the error is in the construction of the camera (in $\mathbf{K}$) or in the camera attitude (in $\mathbf{C}$). It is common practice to hold K_x fixed at the manufacturer's nominal value for the dimension of a pixel, and to hold K_{xy} fixed at zero. Then one can estimate f to account for overall variations in scale, K_y to determine the *aspect ratio* of the pixel grid, and K_{yx} to find the angle between the sample and line axes.

If the optical train contains an odd number of mirrors, the resulting picture will be a mirror image. One can model this reflection by changing the sign of either K_x or K_y.

Camera Calibration

The preceding paragraph alludes to the necessity of determining the parameters of the camera model through calibration. Standard practice is to image a dense star cluster in flight or a special calibration target in the lab. The known coordinates of the stars or of the fiducial points on the calibration target provide a truth model. Comparing the actual image locations to the predicted ones yields the camera parameters through a least-squares adjustment. One obtains better results by taking many pictures, moving the target in the field of view, for then the differential motion of the images relative to one another as a function of (s, l) can provide distortion terms even when the characteristics of the target are not perfectly known. This is the essence of the "overlapping plate method," in which even uncatalogued stars can contribute to the camera model.[11]

The overlapping plate method as implemented at JPL uses the U-D factorized sequential filter,[12] with corrections to the right ascension and declination of each object treated as uncorrelated stochastic parameters. Three camera pointing angles for each picture and the other camera parameters are estimated as well.[13]

DIGITAL PICTURES

The data used by optical navigation consist of *digital pictures* as opposed to analog pictures obtained on film or photographic plates. A digital picture is an array of *data numbers* or "DN values," each of which is intended to measure the amount of light falling on a specific region of a detector (a pixel) at the focal plane of a camera. The actual DN values differ from the ideal due to various kinds of noise. This section describes these noise sources and presents techniques for manipulating digital pictures so that the real work of optical navigation, the image processing, can be more reliable.

Signal in a Pixel

Incoming light has a *specific intensity* $I(\alpha, \delta, \nu, t)$ which is a function of direction (α, δ), frequency ν and time t. The specific intensity can be measured in photons (or joules) m^{-2} sr^{-1} Hz^{-1} s^{-1}. The camera itself introduces a further frequency-dependent attenuation $F(\nu)$, largely because of a filter.

Modern detectors[14] convert some fraction of the incident photons into *photoelectrons*. For instance, the silicon in CCD detectors absorbs light, and the energy of the photons lifts electrons into a conduction band, whence they can be measured. This fraction, the *quantum efficiency*, can also vary with wavelength; call it $Q(\nu)$.

The measured signal $S(s, l)$ in a pixel is thus the incident intensity, as modulated by the camera and detected in the focal plane, integrated over frequency, over the solid angle Ω subtended by that pixel, and over time, and converted to a number of photoelectrons:

$$S(s,l) = A \iiint I(\alpha, \delta, \nu, t)\, F(\nu)\, Q(\nu)\, d\nu\, d\Omega\, dt \tag{20}$$

where A is the *aperture* of the camera. Note that S as written above is measured in electrons.

The DN value has one component directly proportional to S; it is typical to speak of the *gain* g of the analog-to-digital converter in terms of electrons per DN. There is also a positive bias b added, ideally a constant bias, to avoid having negative voltages emanating from the detector. Thus

$$\mathrm{DN}(s,l) = S(s,l)/g + b. \tag{21}$$

Noise in a Pixel

The measured DN values are subject to several kinds of error, or noise, introduced at various steps. The following is not an exhaustive list:

1) *Shot noise* or *photon noise* arises because the flux of photons is discrete, not continuous, and therefore follows a Poisson distribution. The standard deviation is therefore the square root of the number S of photoelectrons. In terms of DN, the shot noise N_s is

$$N_\mathrm{s}(s,l) = \sqrt{S}/g \approx \sqrt{(\mathrm{DN} - b)/g}. \tag{22}$$

2) *Read noise* N_r is introduced during the measurement of the voltage produced by the photoelectrons. This is a property of the detector electronics and is independent of the signal. It can be measured either in electrons or in DN.

3) *Dark current* or *thermal noise* N_d is the spontaneous production of electrons within the detector, even in the absence of light. These are of course indistinguishable from "real" photoelectrons. They obey the same Poisson statistics, and the effect is to add a constant signal with its own contribution to the noise.

4) *Fixed pattern noise* N_f is a systematic variability in dark current, as a function of (s, l). Blemishes in the detector or damage from radiation can cause certain pixels to be "hot," producing far more DN/s than normal. Again, although the average value in a pixel can be obtained through calibration, this average value is also subject to Poisson statistics, so that even after calibration the amount of picture-to-picture variability in a given hot pixel remains noisier than otherwise.

5) *Quantization noise* N_q is the inevitable result of converting a continuous quantity (the voltage from the detector) into the integer DN values. Whether the conversion is done by rounding or by truncating, it introduces a noise of 1/12 DN.

The total noise N in a pixel is the RSS of all these contributing noise sources:

$$N^2 = N_\mathrm{s}^2 + N_\mathrm{r}^2 + N_\mathrm{d}^2 + N_\mathrm{f}^2 + N_\mathrm{q}^2. \tag{23}$$

The *signal-to-noise ratio* S/N is exactly what the term says: the "signal" S arising only from photons, divided by the total noise. An empirical determination takes the difference in DN between the brightest pixel and neighboring "dark sky" to be the signal, and the standard deviation of the sky to be the noise. Images with $S/N > 3$ are almost always usable; images with S/N between 2 and 3 are sometimes good and sometimes not.

Other Error Sources

Not a statistical noise source but still a consideration, charged particles or high-energy photons can impinge on the detector during an exposure. These will ionize some of the atoms in the detector and produce free electrons. The signal they produce varies with the angle of incidence: at normal incidence, a "cosmic ray hit" looks much like a star image, but at near grazing incidence there will be a long trail. The best way to combat cosmic rays is to take two pictures of the same scene; comparing these pictures will reveal their differences, which are presumably the effects of cosmic rays.

Pixel-to-pixel variations in sensitivity, while not strictly "noise," cause an uncalibrated picture of a uniformly bright target to be more variable than otherwise. This effect can be ameliorated with the use of flat fields, described below.

Row-to-row or column-to-column variations in physical size can arise during manufacture. These effects, if present, can affect opnav results: a geometric calibration ignoring this variation will produce only an *average* pixel scale, but the truth may be that most columns are slightly wider than this and every nth column is significantly narrower. The use of an average pixel scale would thus produce systematically wrong s coordinates. The same consideration of course also applies to the height of rows. This error usually amounts to at most a small fraction of a pixel.

Flat Fielding

It is customary, but not always necessary, to correct a raw picture for the pixel-to-pixel variations in sensitivity, dark current, and fixed pattern noise.[15] This process is routinely done for photometric work, where it is important to measure the contribution of the target to the DN as accurately as possible. For positional work, raw and "flattened" (photometrically calibrated) pictures usually give (s, l) measurements which differ very little. The flattening process requires special calibration frames:

1) Take a set of "bias" or zero-second exposures. Combine them, usually by finding the median value of each pixel, to produce as *master bias* picture $\mathbf{B}$.

2) Take a set of "flat" exposures of a uniformly illuminated featureless scene, with the exposure times such that the average DN level is between 1/2 and 3/4 of its maximum value. Combine them as above to produce a *master flat* picture $\mathbf{F}$.

3) If the camera has significant thermal noise (dark current), take a set of "dark" exposures: allow the chip to accumulate charge, but do not open the shutter. Combine these to produce a *master dark* picture $\mathbf{D}$.

4) Remove the bias from the master dark to produce an adjusted master dark $\mathbf{D}'$. This operation is done one pixel at a time:

$$D'_{i,j} = D_{i,j} - B_{i,j}. \tag{24}$$

5) Remove the bias and dark current from the master flat. If the exposure durations of the flat and dark frames are t_F and t_D respectively, create the adjusted master flat $\mathbf{F}'$ pixel by pixel:

$$F'_{i,j} = F_{i,j} - B_{i,j} - (t_\mathrm{F}/t_\mathrm{D})D'_{i,j}. \tag{25}$$

6) The raw picture $\mathbf{P}$, with exposure duration t_P, is then flattened to produce $\mathbf{P}'$:

$$P'_{i,j} = \left[P_{i,j} - B_{i,j} - (t_\mathrm{P}/t_\mathrm{D})D'_{i,j}\right]\left(\langle \mathbf{F}' \rangle / F'_{i,j}\right) \tag{26}$$

where $\langle \mathbf{F}' \rangle$ is the mean of all pixel values in $\mathbf{F}'$.

Background Removal

If flat, bias and dark pictures are not available, one can often remove the background from a picture heuristically. Many opnav pictures contain mostly dark sky, with one or two small targets and a scattering of stars. One can determine the average DN value of sky pixels and subtract that value from every pixel. The "average" here can be the arithmetic mean or the median, but one must take care not to include cosmic ray hits, hot pixels, or real star images.

If the background is not constant, perhaps due to scattered light from a target outside the field of view, one can fit some polynomial function to the sky pixels. A product of Legendre polynomials works well.

As a last resort, one can take many pictures, and for each pixel find its median value and subtract it in each picture. This can work if the camera attitude changes between pictures. As long as every pixel sees sky more often than not, the median value will be a sky pixel. This process can also remove the effects of hot pixels.

IMAGE PROCESSING

The discipline of image processing or image analysis consists of extracting the (s, l) coordinates of an image of a target within a picture. A variety of techniques[16,17] can be brought to bear on the problem, but all of them involve at the most basic level fitting a model of the brightness in each pixel to the measured brightness array. There are many centerfinding techniques, but most of them fall into one of two general categories: correlating the actual image to a pixelated model image, and solving for the parameters of a continuous model of the brightness. One technique which does not fit neatly into either camp is limb scanning, in which points on the *limb* or apparent "edge" of a body are found through correlation and then the center is found by fitting a limb profile to these points.

Centerfinding by Correlation

Let $\mathbf{D}$ be a $d \times d$ array of observed DN values in a portion of a picture which presumably contains an image of a target. Let $\mathbf{P}$ be a $p \times p$ array of predicted DN values. The predicted image location (s_p, l_p) is known by construction. The task of correlation is to locate the brightness pattern in $\mathbf{P}$ within $\mathbf{D}$.

We note that this technique does not depend on the method of constructing $\mathbf{P}$. The predicted array could be a pixelated *point-spread function* if the image is a star. It could be a synthetic image of an entire celestial body, computed pixel by pixel using the known geometry and appropriate reflectance laws. It could be a small patch of terrain on a much larger body. The correlation technique remains the same, even though $\mathbf{P}$ can represent quite different things.

Define the *correlation array* $\rho(\Delta s, \Delta l)$ as the sum of the products of the suitably normalized arrays $\mathbf{D}'$ and $\mathbf{P}'$, with $\mathbf{P}'$ shifted by integer amounts Δs and Δl relative to $\mathbf{D}'$:

$$\rho(\Delta s, \Delta l) = \sum_i \sum_j P'_{i,j} D'_{i+\Delta s, j+\Delta l} \tag{27}$$

where the sum is carried out over only those elements which lie within the bounds of both arrays. In practice, one prefers that $\mathbf{D}$ (typically a subset of a picture) be large enough that $\mathbf{P}$ will completely overlap it for all plausible values of Δs and Δl.

The normalization for $\mathbf{D}$ and $\mathbf{P}$ makes their common portion *zero mean* and *unit standard deviation*. Find the arithmetic mean of all the pertinent elements in each array and subtract it from each element. Then find the RSS of these elements, and divide each element by it.

In practice, the normalization is done after the double summation, and Eq. (27) is evaluated using the

unnormalized arrays. Compute

$$m_d = \sum D_{i+\Delta s, j+\Delta l}, \tag{28}$$

$$s_d = \sum D^2_{i+\Delta s, j+\Delta l}, \tag{29}$$

$$m_p = \sum P_{i,j}, \tag{30}$$

$$s_p = \sum P^2_{i,j}, \tag{31}$$

$$r = \sum D_{i+\Delta s, j+\Delta l}\, P_{i,j}, \tag{32}$$

and then

$$\rho(\Delta s, \Delta l) = \frac{Nr - m_d\, m_p}{\sqrt{(Ns_d - m_d^2)(Ns_p - m_p^2)}} \tag{33}$$

where N is the number of pixels involved in the summation.

The resulting value of ρ will lie between -1 and $+1$, thanks to the normalization; a value of $+1$ indicates a perfect correlation between the two arrays. The value of $(\Delta s, \Delta l)$ for which ρ is a maximum gives the offset in sample and line between the assumed or nominal image location and the location of the peak correlation.

Subpixel accuracy can then be achieved by interpolating the array $\rho(\Delta s, \Delta l)$. One easy method uses a parabolic fit. Let

$$\rho_0 = \rho(\Delta s, \Delta l); \tag{34}$$

$$\rho_- = \rho(\Delta s - 1, \Delta l); \tag{35}$$

$$\rho_+ = \rho(\Delta s + 1, \Delta l). \tag{36}$$

and fit a parabola $y = ax^2 + bx + c$ through the three points $(-1, \rho_-)$, $(0, \rho_0)$ and $(+1, \rho_+)$. By construction ρ_0 is the largest of the three correlation values, so the parabola will open downward $(a < 0)$, and the x coordinate of the vertex yields the interpolated sample coordinate of the correlation peak. A little algebra gives the desired result:

$$x = 2\frac{\rho_+ + \rho_- - 2\rho_0}{\rho_+ - \rho_-}. \tag{37}$$

Similar equations, using the values above and below the peak response, yield the interpolated line coordinate.

The above technique is often called *spatial correlation*, as the shifting is done in pixel coordinates. An alternative is *frequency correlation* using Fast Fourier Transforms of the two arrays. The methods are mathematically equivalent. The FFT is generally preferred if the shift between **P** and **D** can be large, but if the *a priori* image location is not far off the mark, the spacial correlation works just as well.

Centerfinding by Analytic Function Fitting

The second broad class of centerfinding techniques involves fitting some sort of analytic *brightness function* to the DN array. Each DN value is an observation, and a least-squares solution determines the values of the parameters of the fitting function. As the fitting function is not linear, the process is iterative.

The brightness function is a surface density, measured in units of DN per square pixel. The observed DN in a pixel is obtained from photoelectrons generated throughout the light-sensitive or *active region* of that pixel (often, but not always, the entire area of the pixel). The modeled DN must therefore be the integral of the brightness function over the active region.

One simple example is the two-dimensional Gaussian. The brightness function is

$$B(s,l) = \frac{h}{2\pi} \exp\left(-\frac{(s-s_c)^2 + (l-l_c)^2}{2\sigma^2}\right) + b \tag{38}$$

$$\equiv h\, N\left(\frac{s-s_c}{\sigma}\right) N\left(\frac{l-l_c}{\sigma}\right) + b$$

$$\equiv h\, N(\xi(s))\, N(\eta(l)) + b. \tag{39}$$

Here (s_c, l_c) are the coordinates of the peak of the Gaussian, σ is the standard deviation in pixels, h is the amplitude in DN, and b is a constant background in DN. (It is easy enough to make b a function of position as well.) In the last two expressions $N(z)$ is the normal probability distribution function, with zero mean and unit standard deviation; the functions $\xi(s)$ and $\eta(l)$ convert s and l into units of standard deviations away from the mean.

The modeled DN is the integral of the brightness function. If the active region encompasses the entire pixel,

$$\begin{aligned}\mathrm{DN}(s,l) &= \int_{x=s-1/2}^{s+1/2} \int_{y=l-1/2}^{l+1/2} B(x,y)\, dy\, dx \\ &= h\left[\mathrm{erf}(\xi(s+\tfrac{1}{2})) - \mathrm{erf}(\xi(s-\tfrac{1}{2}))\right]\ \left[\mathrm{erf}(\eta(l+\tfrac{1}{2})) - \mathrm{erf}(\eta(l-\tfrac{1}{2}))\right] + b.\end{aligned} \tag{40}$$

Note that Eq. (40) assumes that integer values of s and l are located at the center of the pixel. Other definitions are possible, in which case the limits of the integrals must change. Clearly the limits must also change if the active area is less than the whole pixel.

The fitting process is straightforward. The model parameters are $\{s_c, l_c, h, b, \sigma\}$. Begin with their *a priori* values, perhaps crudely calculated from the image. Use Eq. (40) to calculate the expected DN values in each pixel of a subset of the picture large enough to contain the entire image plus some margin on all sides. Compute the partial derivatives of $\mathrm{DN}(s,l)$ with respect to the solution parameters and form the residuals to construct each equation of condition. Apply a data weight according to the expected noise (in DN), and feed the resulting weighted equation into a least squares algorithm. Iterate, possibly taking partial steps, until convergence is achieved. We have found it useful to hold σ fixed during the first few iterations, then add it to the solution set once (s_c, l_c) have stabilized.

Another widely used *point-spread function* is the Lorentzian function

$$B(s,l) = \frac{h}{1 + (r/r_0)^2} + b, \tag{41}$$

where $r^2 \equiv (s-s_c)^2 + (l-l_c)^2$, r_0 is evidently the *half width at half maximum* of the PSF, and h and b are as before. This function has the advantage that its integral is analytic, even when it is convolved with a line segment to produce a linearly smeared or trailed PSF. The equations for the "smear model" appear in Reference 17 and need not be repeated here.

The Lorentzian function is but a special case of the more general Moffat function,[18] in which the denominator is raised to some arbitrary power. This too is integrable if the exponent is an integer.

Experience has shown that the final values of (s_c, l_c) are not very sensitive to the choice of a reasonable fitting function.

Limb Scanning

Targets whose images span more than a few pixels have historically been analyzed using a *limb scanning* technique.[16] Originally developed because of computer speed and memory limitations, this technique remains in wide use.

The formulation below assumes that the target is a *triaxial ellipsoid*. Define a body-fixed coordinate system B aligned with the principal axes of the ellipsoid, with the z-axis being the axis of rotation and the prime

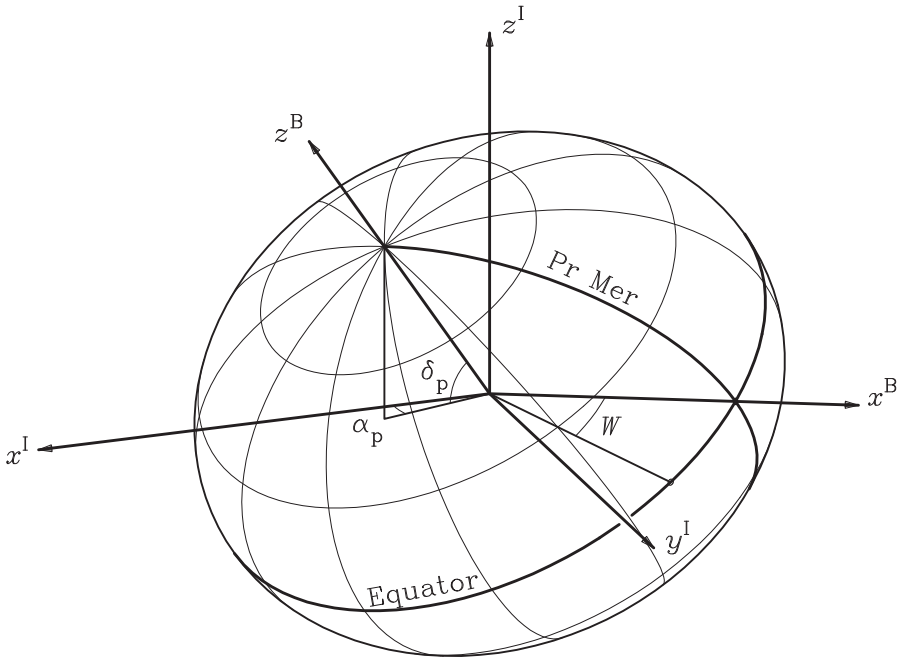

Figure 2. The orientation of a triaxial ellipsoid.

meridian lying in the $+x$-z half-plane (Figure 2). The rotation $\mathbf{B}$ from inertial coordinates to body-fixed coordinates is conventionally[4]

$$\mathbf{B} = \mathbf{R}_3(W)\,\mathbf{R}_1(90^\circ - \delta)\,\mathbf{R}_3(\alpha + 90^\circ) \tag{42}$$

where α and δ are the right ascension and declination of the body's z-axis and W is a rotation angle. All three angles may be functions of time; in the case of uniform rotation,

$$W(t) = W_0 + \omega(t - t_0) \tag{43}$$

while α and δ remain constant.

The equation of the ellipsoid, in body-fixed coordinates, is

$$\frac{x^2}{a^2} + \frac{y^2}{b^2} + \frac{z^2}{c^2} = 1 \tag{44}$$

where a, b and c are the semiaxes of the ellipsoid. We can rewrite Eq. (44) in terms of vectors. Let $\mathbf{p}$ be the vector from the center of the body to a surface point. Define a "shape matrix" $\mathbf{S}$, in body-fixed coordinates, by

$$\mathbf{S} \equiv \begin{pmatrix} 1/a & 0 & 0 \\ 0 & 1/b & 0 \\ 0 & 0 & 1/c \end{pmatrix} \tag{45}$$

and define its square,

$$\mathbf{Q} \equiv \mathbf{S}^{\mathrm{T}}\mathbf{S} = \begin{pmatrix} 1/a^2 & 0 & 0 \\ 0 & 1/b^2 & 0 \\ 0 & 0 & 1/c^2 \end{pmatrix}. \tag{46}$$

Then Eq. (44) becomes

$$(\mathbf{S}\,\mathbf{p})^{\mathrm{T}}\,(\mathbf{S}\,\mathbf{p}) = \mathbf{p}^{\mathrm{T}}\,\mathbf{Q}\,\mathbf{p} = 1. \tag{47}$$

The normal **n** to the surface is found from the gradient of Eq. (44); in body-fixed coordinates,

$$\mathbf{n} = \begin{pmatrix} x/a^2 \\ y/b^2 \\ z/c^2 \end{pmatrix} = \mathbf{Q}\,\mathbf{p}. \tag{48}$$

(We suppress an unnecessary factor of 2; the direction of **p** is all that matters.)

The *limb* of a body is the set of points which, when projected into an image, form the boundary of the image. The surface at these points is always tangent to a line joining the point to the camera; in other words, the direction to the camera is perpendicular to the surface normal. This is a necessary condition, but only for convex bodies is it a sufficient condition. If **A** is the vector from the camera to the *center* of the body, then the limb is the set of points satisfying

$$(\mathbf{A} + \mathbf{p}) \cdot \mathbf{n} = 0. \tag{49}$$

If we substitute Eq. (48) for **n**, this becomes

$$\mathbf{A}^{\mathrm{T}}\,\mathbf{Q}\,\mathbf{p} = -1, \tag{50}$$

which is the equation of a plane.

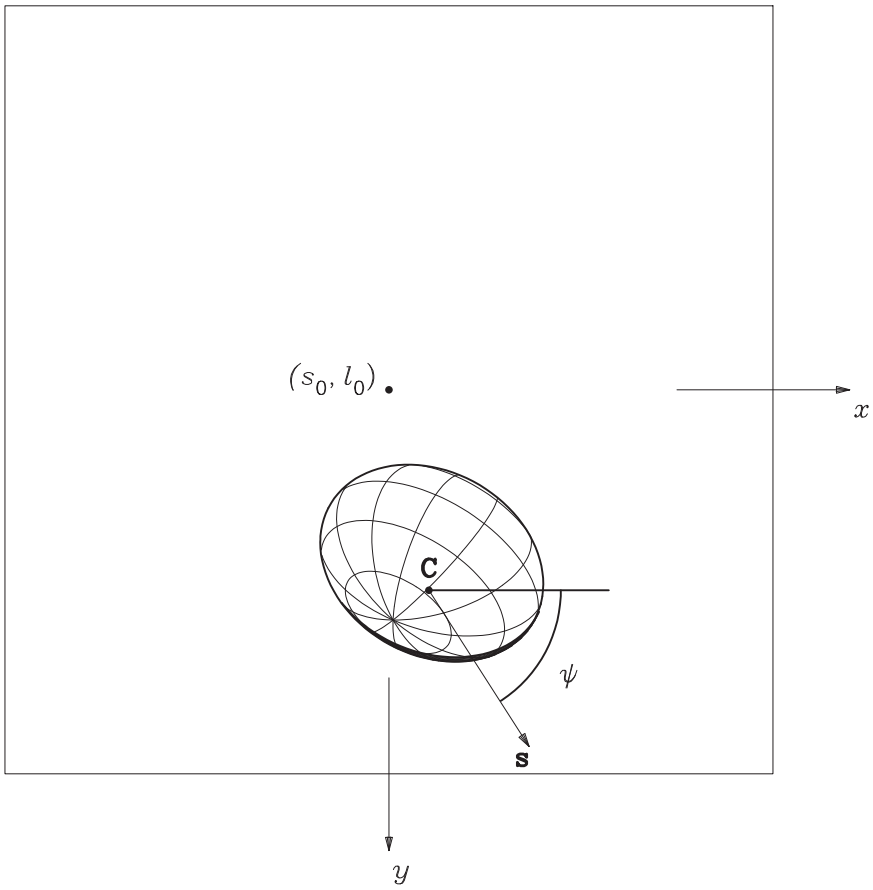

Figure 3. A scan vector shown on a picture of an ellipsoid.

The limb scanning process (Figure 3) involves examining the actual and predicted brightness levels along a *scan line* in the picture. This is a ray, emanating from a *scan center* C at some *scan angle* ψ. The scan

center need not correspond to the actual or predicted center of the body. In camera coordinates, the scan center vector is

$$\mathbf{C} = \begin{pmatrix} x_0 \\ y_0 \\ f \end{pmatrix}. \tag{51}$$

We also define the *scan vector*

$$\hat{\mathbf{s}} = \begin{pmatrix} \cos\psi \\ \sin\psi \\ 0 \end{pmatrix}. \tag{52}$$

The scan center and scan vector together define a *scan plane* in space, which projects into a scan line in the picture. Any vector $\mathbf{x}$ will lie in the scan plane if

$$(\mathbf{C} \times \hat{\mathbf{s}}) \cdot \mathbf{x} = 0. \tag{53}$$

A limb point $\mathbf{p}$ must therefore satisfy simultaneously the quadratic Eq. (47), the linear Eq. (50), and the linear Eq. (53), with $\mathbf{A} + \mathbf{p}$ substituted for $\mathbf{x}$ in the last of these. The two linear equations define two planes; their intersection is a line; the line intersects the ellipsoid in two points if $\mathbf{C}$ is properly chosen; the point with $\mathbf{p} \cdot \hat{\mathbf{s}} > 0$ is the preferred solution.

Note that Eqs. (47) and (50) are vector equations and therefore valid in any coordinate system, although the components of Q given in Eq. (46) take this simple form only in body-fixed coordinates. We can express these equations in any other coordinate system—in particular, camera coordinates—as follows.

Let T be the rotation matrix which transforms from body-fixed coordinates into camera coordinates:

$$\mathsf{T} = \mathsf{C}\,\mathsf{B}^{-1} = \mathsf{C}\,\mathsf{B}^{\mathrm{T}}. \tag{54}$$

Multiply each occurrence of $\mathbf{p}$ on the left-hand side of Eq. (47) by $(\mathsf{T}^{\mathrm{T}}\,\mathsf{T})$, which is the identity matrix, and rearrange terms:

$$(\mathbf{p}^{\mathrm{B}})^{\mathrm{T}}\,\mathsf{Q}^{\mathrm{B}}\,\mathbf{p}^{\mathrm{B}} = ((\mathsf{T}^{\mathrm{T}}\,\mathsf{T})\,\mathbf{p}^{\mathrm{B}})^{\mathrm{T}}\,\mathsf{Q}^{\mathrm{B}}\,(\mathsf{T}^{\mathrm{T}}\,\mathsf{T})\,\mathbf{p}^{\mathrm{B}} \tag{55}$$

$$= (\mathsf{T}\,\mathbf{p}^{\mathrm{B}})^{\mathrm{T}}\,(\mathsf{T}\,\mathsf{Q}^{\mathrm{B}}\,\mathsf{T}^{\mathrm{T}})\,(\mathsf{T}\mathbf{p}^{\mathrm{B}}) \tag{56}$$

$$= (\mathbf{p}^{\mathrm{C}})^{\mathrm{T}}\,\mathsf{Q}^{\mathrm{C}}\,\mathbf{p}^{\mathrm{C}} = 1. \tag{57}$$

Now the left-hand side is expressed in camera coordinates, and we have rotated Q into camera coordinates as well. The same transformation can also be applied to Eq. (50). As Eq. (53) was already specified in camera coordinates, we now have three vector equations, all expressed in the same coordinate system, which can be solved for $\mathbf{p}$.

If the vector $\mathbf{A}$ be replaced by the direction to the sun, the same formulation yields the *terminator*, the set of points which divide lit surface from unlit.

The above formulation is specific to triaxial ellipsoids, of which spheres and spheroids are special cases. Small bodies in particular are not well modeled by ellipsoids. One approach is to determine a dense grid of points on the surface and connect them with line segments to form a set of triangular *plates*. Another is to represent the length of the radius vector r as an arbitrary function of body-centered latitude φ and longitude λ, for instance as the sum of spherical harmonics:

$$r(\lambda,\varphi) = \sum_{n=0}^{N} \sum_{m=0}^{n} P_{nm}(\sin\varphi)(a_{nm}\cos m\lambda + b_{nm}\sin m\lambda). \tag{58}$$

Regardless of the shape model, the vector $(\mathbf{A} + \mathbf{p})$, from the camera to some spot on the surface of the body, can be projected into the picture as for any other vector. Similarly, a point (s, l) in the picture can be converted into a vector, and the intersection of that vector with the surface can be determined.

The process of limb scanning proceeds as follows.

1) Begin with an assumed (s_c, l_c) of the center of the body. This yields the scan center vector **C**.

2) Determine a set of scan angles ψ based on the apparent size of the body. For each scan angle,

a) determine the limb or terminator point which lies in the scan plane for this scan angle. Not all scan angles will necessarily give usable points. Terminator points and the unlit limb which lies beyond the terminator may be discarded. The limb point will have some nominal (s, l) coordinates in the picture and a vector **p** in space.

b) In the picture, determine (using bilinear interpolation or otherwise) the observed DN values along the scan line: one at the nominal limb point, the rest equally spaced in pixels on either side of the nominal point. The result is a one-dimensional array of observed DN.

c) Project each of these points onto the body if possible. For each point, determine the angle of incidence i, the angle of emission e, and the phase angle ϕ. Use these angles, with the albedo of the surface at that point and some appropriate reflectance law, to determine the expected brightness from the surface. The result is a one-dimensional array of expected DN values, many of which will be zero.

d) Perform a one-dimensional correlation of the expected and observed DN values, which yields the offset of the observed limb from the nominal limb at this scan angle.

3) After all the scan angles have been processed, the observed offsets go into a least-squares fit to solve for (s_c, l_c) and perhaps parameters governing the shape of the body as well.

4) Iterate steps 2 and 3 until convergence is achieved.

Moment Algorithm

The most primitive of all the centerfinding methods is the moment algorithm, which simply determines the center of brightness of an array:

$$s_c = \frac{\sum_i \sum_j i \, \mathrm{DN}_{i,j}}{\sum_i \sum_j \mathrm{DN}_{i,j}}; \tag{59}$$

$$l_c = \frac{\sum_i \sum_j j \, \mathrm{DN}_{i,j}}{\sum_i \sum_j \mathrm{DN}_{i,j}}. \tag{60}$$

This method must be used with care. The presence of a uniform nonzero background will cause (s_c, l_c) to move toward the center of the DN array, so the background must be carefully removed. Noise spikes far from the image will have a disproportionate effect on the results, so these must be removed as well. One quick cure for these problems is to exclude from the sums all pixels whose DN value is less than some minimum percentage of the brightest pixel in the image.

Manual Registration

When all else fails, the human eyes and the brain behind them remain a potent vehicle for determining the center of an image. Missions from NEAR Shoemaker to Stardust have used opnav data based on manual centerfinding.

PARTIAL DERIVATIVES

Image processing, described in the previous section, produces the *observed* coordinates (s_c, l_c) of images of targets. These measurements must then be passed to an orbit determination filter, along with the radiometric tracking data and *a priori* constraints on the target ephemeris, so that the state of the spacecraft may be estimated. The estimation process can also include corrections to the target ephemeris. We therefore require residuals and partial derivatives in order to form the equations of condition for the optical data. The computation of the expected image coordinates follows exactly the same methods which were used to predict the

coordinates initially, although usually using better values for the camera pointing angles. (It is customary for the opnav analyst to estimate the pointing angles offline immediately after the centerfinding is complete.)

The partial derivatives (see References 16 and 17) may be found by differentiating Eqs. (1) through (18). The parameters fall into several categories:

1) *Dynamic parameters* affect the spacecraft trajectory. These include the initial position and velocity of the spacecraft; the position, velocity and mass of perturbing bodies; maneuvers; and other nongravitational accelerations. The vectors $\mathbf{R}(t)$ and $\dot{\mathbf{R}}(t)$ will therefore have nonzero partials with respect to these parameters, and the partials will propagate into τ, $\mathbf{T}(t)$, $\mathbf{A}(t)$, and then into sample and line.

2) *Target parameters* affect the position and velocity of the target. Orbital elements, masses, and for stars the coordinates and proper motion, are examples. (Some of these may affect the spacecraft too.) These affect $\mathbf{S}(t)$, and the partials propagate into τ, $\mathbf{T}(t)$, $\mathbf{A}(t)$ and (s, l) as above.

3) *Optical parameters* affect the transformation from $\mathbf{A}(t)$ into sample and line. They do not affect the spacecraft trajectory, nor the target ephemeris. They do, however, affect the measurements. Examples include the camera focal length f, the components of K, the distortion parameters, and the camera pointing angles however defined.

4) *Optical bias parameters* are intended to soak up systematic errors in the centerfinding process. Typically these are applied to body centers but not to stars.

Partials of Dynamic and Target Parameters

Let q denote some parameter which may affect $\mathbf{R}(t)$ or $\mathbf{S}(t-\tau)$ and therefore $\mathbf{A}(t)$, the apparent position of the target at the time of observation. The partials $\partial\mathbf{R}/\partial q$ and $\partial\mathbf{S}/\partial q$ may be interpolated from files or calculated analytically; this paper assumes that their values are available somehow.

Begin by differentiating Eq. (2):

$$\frac{\partial\mathbf{T}}{\partial q} = \frac{\partial\mathbf{S}(t-\tau)}{\partial q} - \frac{\partial\mathbf{R}(t)}{\partial q} - \frac{\partial\mathbf{S}(t-\tau)}{\partial(t-\tau)}\,\frac{\partial\tau}{\partial q}. \tag{61}$$

Because $\tau = |\mathbf{T}|/c$,

$$\frac{\partial\tau}{\partial q} = \frac{1}{c}\,\frac{\partial|\mathbf{T}|}{\partial q} = \frac{1}{c}\left(\hat{\mathbf{T}}\cdot\frac{\partial\mathbf{T}}{\partial q}\right). \tag{62}$$

Once again we have the desired quantity, this time $\partial\mathbf{T}/\partial q$, on both sides of the equation. Now, however, there is an exact solution:

$$\frac{\partial\mathbf{T}}{\partial q} = \frac{\partial\mathbf{S}(t-\tau)}{\partial q} - \frac{\partial\mathbf{R}(t)}{\partial q} - \frac{\dot{\mathbf{S}}(t-\tau)}{c}\,\frac{\dot{\mathbf{T}} - \partial(\mathbf{S}(t-\tau)-\mathbf{R}(t))/\partial q}{1+(\dot{\mathbf{S}}\cdot\dot{\mathbf{T}})/c}. \tag{63}$$

The next step is to differentiate Eq. (3):

$$\frac{\partial\mathbf{A}}{\partial q} = \frac{\partial\mathbf{T}}{\partial q} + \frac{\dot{\mathbf{R}}(t)}{c}\left(\dot{\mathbf{T}}\cdot\frac{\partial\mathbf{T}}{\partial q}\right) + \frac{|\mathbf{T}|}{c}\,\frac{\partial\dot{\mathbf{R}}(t)}{\partial q}. \tag{64}$$

The above partials are presumably calculated in inertial coordinates. They must then be rotated into camera coordinates:

$$\frac{\partial\mathbf{A}^{\mathrm{C}}}{\partial q} = \mathsf{C}\frac{\partial\mathbf{A}^{\mathrm{I}}}{\partial q} + \frac{\partial\mathsf{C}\mathbf{A}^{\mathrm{I}}}{\partial q}. \tag{65}$$

The dynamic parameters usually propagate only through the first term; the second term handles the various pointing angles which define C.

Next, transform $\partial\mathbf{A}^{\mathrm{C}}/\partial q$ into the focal plane:

$$\begin{pmatrix}\partial x/\partial q\\ \partial y/\partial q\end{pmatrix} = \frac{f}{A_3^{\mathrm{C}}}\begin{pmatrix}\partial A_1^{\mathrm{C}}/\partial q\\ \partial A_2^{\mathrm{C}}/\partial q\end{pmatrix} - \frac{f}{(A_3^{\mathrm{C}})^2}\begin{pmatrix}A_1^{\mathrm{C}}\\ A_2^{\mathrm{C}}\end{pmatrix}\frac{\partial A_3^{\mathrm{C}}}{\partial q}. \tag{66}$$

Then find the partials of the distortion corrections,

$$\begin{pmatrix} \partial\Delta x/\partial x \\ \partial\Delta x/\partial y \\ \partial\Delta y/\partial x \\ \partial\Delta y/\partial y \end{pmatrix} = \begin{pmatrix} r^2+2x^2 & y & 2x \\ 2xy & x & 0 \\ 2xy & 0 & y \\ r^2+2y^2 & 2y & x \end{pmatrix} \begin{pmatrix} \epsilon_1 \\ \epsilon_2 \\ \epsilon_3 \end{pmatrix}, \tag{67}$$

and use these to get the partials with respect to any parameter via the chain rule:

$$\begin{pmatrix} \partial\Delta x/\partial q \\ \partial\Delta y/\partial q \end{pmatrix} = \begin{pmatrix} \partial\Delta x/\partial x & \partial\Delta x/\partial y \\ \partial\Delta y/\partial x & \partial\Delta y/\partial y \end{pmatrix} \begin{pmatrix} \partial x/\partial q \\ \partial y/\partial q \end{pmatrix}. \tag{68}$$

This gives the partials of the corrected position (x', y'):

$$\begin{pmatrix} \partial x'/\partial q \\ \partial y'/\partial q \end{pmatrix} = \begin{pmatrix} \partial x/\partial q \\ \partial y/\partial q \end{pmatrix} + \begin{pmatrix} \partial\Delta x/\partial q \\ \partial\Delta y/\partial q \end{pmatrix}. \tag{69}$$

Finally, the partials of sample and line come from differentiating Eq. (18):

$$\begin{pmatrix} \partial s/\partial q \\ \partial l/\partial q \end{pmatrix} = \mathbf{K} \begin{pmatrix} \partial x'/\partial q \\ \partial y'/\partial q \end{pmatrix}. \tag{70}$$

Partials of Optical Parameters

These are found by differentiating the appropriate equations, this time with respect to the parameters which appear explicitly in them.

For focal length f,

$$\begin{pmatrix} \partial x/\partial f \\ \partial y/\partial f \end{pmatrix} = \frac{1}{A_3^{\mathrm{C}}} \begin{pmatrix} A_1^{\mathrm{C}} \\ A_2^{\mathrm{C}} \end{pmatrix}. \tag{71}$$

These partials are then transformed into $\partial(s,l)/\partial f$ by Eqs. (68) through (70).

For the distortion coefficients, obviously

$$\frac{\partial(x',y')}{\partial(\epsilon_1,\epsilon_2,\epsilon_3)} = \frac{\partial(\Delta x,\Delta y)}{\partial(\epsilon_1,\epsilon_2,\epsilon_3)} = \begin{pmatrix} xr^2 & xy & x^2 \\ yr^2 & y^2 & xy \end{pmatrix}, \tag{72}$$

and again these are converted to sample and line via Eq. (70).

For the components of $\mathbf{K}$,

$$\frac{\partial(s,l)}{\partial(K_x,K_{yx},K_{xy},K_y)} = \begin{pmatrix} x' & 0 & y' & 0 \\ 0 & x' & 0 & y' \end{pmatrix} \tag{73}$$

with no further transformation required.

Partials with respect to (s_0, l_0) are trivial, but these parameters are seldom estimated. Rather, it is convenient to hold them fixed at the center of the detector. If the actual location of the optical axis differs from this, the distortion terms ϵ_2 and ϵ_3 can soak up the difference.

Partials with respect to pointing angles are found by differentiating the matrix $\mathbf{C}$ with respect to these angles. These partials enter into the second term on the right-hand side of Eq. (65).

Partials of Optical Bias Parameters

We have seen above that it can be a difficult task to determine the image coordinates of the center of a body. Limb scanning results can be affected by scattered light, by an incorrect reflectance law, or by a mismodeling of the body's shape. For instance, if a body is more oblate than the model, the equator will be further than

expected from the body's rotational axis, and fitting the wrong shape for the limb will pull the inferred center away from the spin axis. Errors in the reflectance law can easily produce an error in the sunward direction. Comets pose a special problem, because the nucleus is far smaller than the observable coma, and the coma itself is likely to have a sunward bias. For these reasons it is convenient and sometimes necessary to introduce optical bias parameters.

There are typically three kinds of optical bias.

1) A constant bias in camera coordinates may arise from a frame-tie error or other problems with the star catalog. There are two such parameters, b_s and b_l, one in sample and one in line. Obviously $\partial s/\partial b_s = 1$ and $\partial l/\partial b_l = 1$, and the cross partials are zero. These partials are zero, by definition, for stars.

2) A bias proportional to the apparent diameter of the body may arise from systematic topography variations or other physical effects. This effect is really measured in kilometers, not in pixels. If the diameter of the target body is D, the partials are $FK_xD/|\mathbf{T}|$ in the sample direction and $FK_yD/|\mathbf{T}|$ in the line direction.

3) A bias like 2) but acting in the sunward direction, with a magnitude depending somehow on the phase angle. One determines the direction to the sun in the image and sets up a partial in that direction. Often the phase dependence can be expressed as a power of $\sin(\phi/2)$.

These biases are most useful in covariance studies, but they can also be used to force the optical residuals to lie flat.

CONCLUSION

Space limitations prevent this paper from being a full treatise on the mathematical methods of optical navigation. The uses of optical navigation are diverse, as it deals with targets ranging in size from centimeters to thousands of kilometers; with cameras whose field of view can vary over an order of magnitude; with all kinds of detectors, with cameras on spacecraft or telescopes in observatories. The same underlying geometry applies to everything, but the methods of extracting positional information from pictures vary widely from case to case. What is presented here is therefore more of a primer, an appetizer, an invitation to the readers to work through the equations for themselves, to find new ways of coaxing navigation information out of pictures.

ACKNOWLEDGMENTS

The techniques described in this paper have been developed more or less continuously since the mid-1960s;[1] I have merely gathered the most important material into one place. Tom Duxbury, Chuck Acton, and the late Bill Breckenridge were among the pioneers who devised the nomenclature and basic methods which are still in use today. Steve Synnott, Joe Donegan, Ed Riedel, Juli Stuve, Robin Vaughan, Shyam Bhaskaran, Mike Wang, Bob Werner and Brian Rush have contributed algorithms or source code. I am indebted to all of them.

The research described in this paper was carried out at the Jet Propulsion Laboratory, California Institute of Technology, under a contract with the National Aeronautics and Space Administration.

REFERENCES

[1] W. M. Owen, Jr., T. C. Duxbury, C. H. Acton, Jr., S. P. Synnott, J. E. Riedel and S. Bhaskaran, "A Brief History of Optical Navigation at JPL," AAS paper 08–053, 31st Annual AAS Guidance and Control Conference, Breckenridge, CO, February 2008.

[2] S. Bhaskaran, S. D. Desai, P. J. Dumont, B. M. Kennedy, G. W. Null, W. M. Owen, Jr., J. E. Riedel, S. P. Synnott and R. A. Werner, "Orbit Determination Performance Evaluation of the Deep Space 1 Autonomous Navigation Systen," AAS paper 98–193, AAS/AIAA Spaceflight Mechanics Meeting, Monterey, CA, February 1998.

[3] A. König, "Astronomy with Astrographs," in *Astronomical Techniques* (W. A. Hiltner, ed.), University of Chicago Press, 1962, pp. 401–486.

[4] P. K. Seidelmann *et al.*, *Explanatory Supplement to the Astronomical Almanac*, University Science Books, 1992.

[5] P. Stumpff, "On the Relationship between Classical and Relativistic Theory of Stellar Aberration," *Astronomy and Astrophysics* **84**, 257–259, 1980,

[6] European Space Agency, *The Hipparcos and Tycho Catalogues: Astrometric and Photometric Star Catalogues derived from the ESA Hipparcos Space Astrometry Mission*, ESA publication SP–1200, June 1997.

[7] E. Høg, C. Fabricius, V. V. Makarov, S. Urban, T. Corbin, G. Wycoff, U. Bastian, P. Schwekendiek and A. Wicenec, "The Tycho-2 Catalogue of the 2.5 Million Brightest Stars," *Astronomy and Astrophysics* **355**, L27–L30, 2000,

[8] N. Zacharias, S. E. Urban, M. I. Zacharias, G. L. Wycoff, D. M. Hall, D. G. Monet and T. J. Rafferty, "The Second U. S. Naval Observatory CCD Astrograph Catalog (UCAC2)," *Astronomical Journal* **127**, 3043–3059, 2004.

[9] D. J. Schroeder, *Astronomical Optics*, second edition, Academic Press, 1999.

[10] F. Jenkins and H. White, *Fundamentals of Optics*, McGraw-Hill, 1957.

[11] H. K. Eichhorn, "Über die Reduktion von photographischen Sternpositionen und Eigenbewegungen," *Astronomische Nachrichten* **285**, 233–237, 1960.

[12] G. J. Bierman, *Factorization Methods for Discrete Sequential Estimation*, Academic Press, 1977.

[13] W. M. Owen, Jr., S. P. Synnott and G. W. Null, "High-Accuracy Asteroid Astrometry from Table Mountain Observatory," in *Modern Astrometry and Astrodynamics* (R. Dvorak, H. F. Haupt and K. Wodnar, eds.), Verlag der Österreichischen Akademie der Wissenschaften, Vienna, 1998, pp. 89–102.

[14] M. J. Eccles, M. E. Sim and K. P. Tritton, *Low Light Level Detectors in Astronomy*, Cambridge University Press, 1983.

[15] S. B. Howell, *Handbook of CCD Astronomy*, Cambridge University Press, 2000.

[16] S. P. Synnott, A. J. Donegan, J. E. Riedel and J. A. Stuve, "Interplanetary Optical Navigation: Voyager Uranus Encounter," AIAA paper 86–3113, AIAA/AAS Astrodynamics Conference, Williamsburg, VA, August 1986.

[17] J. E. Riedel, W. M. Owen, Jr., J. A. Stuve, S. P. Synnott and R. M. Vaughan, "Optical Navigation During the Voyager Neptune Encounter," AIAA paper 90–2877, AIAA/AAS Astrodynamics Conference, Portland, OR, August 1990.

[18] A. F. J. Moffat, "A Theoretical Investigation of Focal Stellar Images in the Photographic Emulsion and Application to Photographic Photometry," *Astronomy and Astrophysics* **3**, 455–461, 1969.